

## Evidence That Highly Conserved Residues of Transmembrane Segment 6 of *Escherichia coli* MntH Are Important for Transport Activity<sup>†</sup>

Heather A. H. Haemig, Patrick J. Moen, and Robert J. Brooker\*

*Department of Genetics, Cell Biology, and Development, University of Minnesota, 321 Church Street, Minneapolis, Minnesota 55455*

*Received March 3, 2010; Revised Manuscript Received April 28, 2010*

**ABSTRACT:** Nramp (natural resistance-associated macrophage protein) family members have been characterized in mammals, yeast, and bacteria as divalent metal ion/H<sup>+</sup> symporters. In previous work, a bioinformatic approach was used for the identification of residues that are conserved within the Nramp family [Haemig, H. A., and Brooker, R. J. (2004) *J. Membr. Biol.* **201** (2), 97–107]. On the basis of site-directed mutagenesis of highly conserved negatively charged residues, a model was proposed for the metal binding site of the *Escherichia coli* homologue, MntH. In this study, we have focused on the highly conserved residues, including two histidines, of transmembrane segment 6 (TMS-6). Multiple mutants were made at the eight conserved sites (i.e., Gly-205, Ala-206, Met-209, Pro-210, His-211, Leu-215, His-216, and Ser-217) in TMS-6 of *E. coli* MntH. Double mutants involving His-211 and His-216 were also created. The results indicate the side chain volume of these residues is critically important for function. In most cases, only substitutions that are closest in side chain volume still permit transport. In addition, the  $K_m$  for metal binding is largely unaffected by mutations in TMS-6, whereas  $V_{max}$  values were decreased in all mutants characterized kinetically. Thus, these residues do not appear to play a role in metal binding. Instead, they may comprise an important face on TMS-6 that is critical for protein conformational changes during transport. Also, in contrast to other studies, our data do not strongly indicate that the conserved histidine residues play a role in the pH regulation of metal transport.

The first member of the Nramp<sup>1</sup> family was identified in the early 1990s as a gene conferring host resistance to a number of pathogenic microorganisms (2). Since then, members of this family of divalent metal ion transporters have been shown to have many important functions in metal ion homeostasis, including dietary iron uptake (3), recycling of red blood cells (4), immune response to pathogenic bacteria (5), and virulence of pathogenic bacteria (6, 7). Nramp family members transport divalent metal cations such as Fe<sup>2+</sup> and Mn<sup>2+</sup> into the cell, coupled with the movement of hydrogen ions (3). Transporters that belong to the Nramp family have been identified in organisms ranging from bacteria to humans, with a preference for transporting iron among eukaryotes and manganese in prokaryotic species (3, 7–11).

In bacteria, the physiological role of an Mn<sup>2+</sup> transporter was first proposed by Silver et al. in the 1970s (12). In *Escherichia coli*, a gene encoding such a manganese transporter, designated *mntH*, was first characterized by two independent groups in 2000 (9, 10). The *mntH* gene was found to be homologous to mammalian Nramp genes. However, the gene was named *mntH*, because the encoded protein, MntH, was found to transport manganese as its

preferred substrate (9, 10). Topology analysis of this protein suggests that there are 11 transmembrane segments (1, 13).

Naturally occurring Nramp mutations in mice and rats (G185R) are known to inhibit function and thereby lead to defects in the dietary absorption of iron and the ability to resist infection by various bacterial pathogens (14–16). Because of its expression in macrophages, many researchers have searched for an association between Nramp1 and autoimmune or infectious diseases. Though more work is necessary, a 5'(GT)<sub>n</sub> promoter polymorphism has been found in diseases such as rheumatoid arthritis, multiple sclerosis, and meningococcal meningitis (reviewed in ref 17). In addition, evidence points to iron's key role in the onset, progression, and outcome of bacterial infections (reviewed in refs 18 and 19), and competition between Nramp homologues may play an important role in pathogenesis (5).

A few mutagenesis studies of Nramp homologues have examined the roles of several highly conserved negatively charged residues in the family (1, 20–23). Of particular interest to our laboratory is the DPGN motif, which is nearly 100% conserved across the family and is found in TMS-1. Of 10 mutations to this region in the *E. coli* MntH homologue, only one (P35G) still maintained Mn<sup>2+</sup> transport levels above background, suggesting a functionally important role for this motif (1). In addition, several highly conserved acidic residues are found within transmembrane segments 1 and 3. Even conservative substitutions (i.e., Glu → Asp) of these charged residues (Glu-102, Asp-109, and Glu-112) resulted in Mn<sup>2+</sup> transport levels that were < 10% of the wild-type MntH level or no transport activity for Mn<sup>2+</sup>. From this work, we proposed a model for the metal binding site (1). According to this model, the metal binding site includes

<sup>†</sup>This work was supported by a seed grant from the Biotechnology Institute of the University of Minnesota. H.A.H.H. has been supported by National Institutes of Health Biotechnology Training Grant IT32-GM08347.

\*To whom correspondence should be addressed. Telephone: (612) 624-3053. E-mail: brook005@umn.edu. Fax: (612) 626-6140.

<sup>1</sup>Abbreviations: Nramp, natural resistance-associated membrane protein; TMS, transmembrane segment; MES, 2-(*N*-morpholino)ethanesulfonic acid; TES, *N*-tris(hydroxymethyl)methyl-2-aminoethanesulfonic acid; TPCK, tosyl phenylalanyl chloromethyl ketone; PMSF, phenylmethanesulfonyl fluoride; SEM, standard error of the mean.

three negatively charged residues (Asp-34, Asp-109, and Glu-112) and four other nearby residues (Pro-35, Gly-36, Asn-37, and Gly-115), all of which are 100% conserved in the Nramp family.

During our sequence comparisons of Nramp family members, we also found several highly conserved residues in TMS-6, including two histidine residues. Histidine pairs have often been cited in the literature as metal binding sites in soluble (24) and membrane proteins (25, 26). In recent mutagenesis studies of the conserved histidine residues of TMS-6, the histidine residues (His-211 and His-216 of *E. coli* MntH and the analogous residues in mouse Nramp2) were proposed to play a role in pH regulation of metal transport (20, 21). However, neither of these studies examined the six additional highly conserved residues in this helix. In this study, we have introduced multiple substitutions of these residues in *E. coli* MntH TMS-6: Gly-205, Ala-206, Met-209, Pro-210, Leu-215, and Ser-217. In addition, we have introduced four substitutions of each histidine (His-211 and His-216) and created four double mutant proteins for analysis. The site-directed mutants were then analyzed with regard to their effects on expression and transport. Mutations affecting the two conserved histidine residues were also examined with regard to a possible role in the pH regulation of metal transport.

## MATERIALS AND METHODS

**Reagents.**  $\text{MnCl}_2$ , MES [2-(*N*-morpholino)ethanesulfonic acid], and TES [N-tris(hydroxymethyl)methyl-2-aminoethanesulfonic acid] were purchased from Sigma (St. Louis, MO).  $^{54}\text{Mn}$  was purchased from Perkin-Elmer (Boston, MA). Restriction enzymes and DNA ligase were purchased from New England Biolabs (Beverly, MA). The QuikChange kit was purchased from Stratagene (La Jolla, CA). All remaining reagents were of analytical grade.

**Bacterial Strains and Methods.** The relevant genotypes of the bacterial strains and mutant plasmids are described in Table 1. Plasmid DNA was purified using the Eppendorf Plasmid Mini DNA Kit (Westbury, NY). Restriction digests and ligations were performed according to the manufacturer's recommendations. Cell cultures were grown in YT medium (27) supplemented with chloramphenicol (30  $\mu\text{g/mL}$ ).

**Site-Directed Mutagenesis.** Mutants were created using the strategies outlined in the QuikChange mutagenesis kit. The entire *mntH* coding region was sequenced to confirm each mutation. The mutations are listed in Table 1.

**$\text{Mn}^{2+}$  Transport Assays.** Cells were grown at 37 °C with shaking to midlog phase in YT medium supplemented with 15  $\mu\text{g/mL}$  chloramphenicol and 0.25 mM isopropyl 1-thio- $\beta$ -D-galactopyranoside. The cells were pelleted by centrifugation at 5000g for 5 min, and the resulting pellet was washed in 50 mM MES buffer (pH 6.0) and then resuspended in the same buffer at a concentration of approximately 0.5 mg of protein/mL. The cells were then diluted 100-fold in the same buffer and equilibrated at 37 °C for 5–10 min before  $^{54}\text{MnCl}_2$  (5  $\mu\text{Ci/mL}$ ) was added. Aliquots of 200  $\mu\text{L}$  were removed at appropriate time points, and the cells were captured on 0.45  $\mu\text{m}$  Metrical membranes (Gelman Sciences, Inc., Ann Arbor, MI). The cells were then washed with 5–10 mL of ice-cold 50 mM MES buffer by rapid filtration. The filter with the cells was then placed in liquid scintillation fluid and counted using a Beckman LS1801 liquid scintillation counter. Channels 401–945 were used to detect photons derived from  $\gamma$ -radiation of  $^{54}\text{Mn}^{2+}$ .

Table 1: Bacterial Strains and Plasmids

strain	relevant characteristics	ref
MM2115	strain MM1925 [ <i>E. coli</i> K12 wild-type $\text{F}^-/\lambda\text{mbda}^-/\text{IN}(\text{rrnD-rrnE})$ ] with a $\text{kan}^R$ insertion in the <i>mntH</i> gene	10
plasmid	description	ref
pSU2718	hybrid pACYC184/pUC18 cloning vector with a chloramphenicol resistance marker and <i>lac</i> promoter	28
p6HmntH	pSU2718, with the wild-type <i>mntH</i> gene under the control of the <i>lac</i> promoter and a six-histidine tag located at the amino terminus of MntH	1
mutation <sup>a</sup>	codon change	protein expression (% of wild-type) <sup>b</sup>
G205A	GGG to GCC	102.0 $\pm$ 11
G205P	GGG to CCG	99.8 $\pm$ 2
A206G	GCG to GGC	87.3 $\pm$ 4
A206L	GCG to CTG	80.1 $\pm$ 5
M209I	ATG to ATC	87.2 $\pm$ 9
M209K	ATG to AAA	80.6 $\pm$ 12
P210A	CCG to GCC	81.8 $\pm$ 11
P210G	CCG to GGG	77.8 $\pm$ 6
P210Q	CCG to CAA	77.7 $\pm$ 5
H211A	CAT to GCT	61.0 $\pm$ 8
H211C	CAT to TGT	67.7 $\pm$ 12
H211Q	CAT to CAG	82.1 $\pm$ 7
H211R	CAT to CGC	80.0 $\pm$ 11
L215A	TTG to GCG	88.3 $\pm$ 7
L215I	TTG to ATC	74.0 $\pm$ 28
L215V	TTG to GTC	80.7 $\pm$ 12
H216A	CAC to GCC	86.3 $\pm$ 10
H216C	CAC to TGC	82.3 $\pm$ 9
H216Q	CAC to CAG	93.8 $\pm$ 9
H216R	CAC to CGG	81.8 $\pm$ 2
S217A	TCC to GCG	84.1 $\pm$ 6
S217Q	TCC to CAG	79.2 $\pm$ 1
S217T	TCC to ACG	77.2 $\pm$ 46
S217Y	TCC to TAT	75.4 $\pm$ 2
H211A/H216A	see the single mutant	90.7 $\pm$ 10
H211C/H216C	see the single mutant	85.8 $\pm$ 44
H211Q/H216Q	see the single mutant	81.1 $\pm$ 36
H211R/H216R	see the single mutant	78.5 $\pm$ 31

<sup>a</sup>The designated mutations were made using plasmid p6HmntH as the starting material. <sup>b</sup>Expression levels were measured in strain MM2115 containing the plasmid with the wild-type *6HmntH* gene or a *6HmntH* gene with the designated mutation as described in Materials and Methods.

As a negative control, strain MM2115/pSU2718, which lacks a functional *mntH* gene, was also subjected to  $\text{Mn}^{2+}$  transport assays (10, 28). The background values from the MM2115/pSU2718 strain were subtracted from the values obtained from the strains carrying the wild-type or mutant *6HmntH* genes. For the experiments depicted in Figures 4 and 5, a 50 mM MES buffer was also used and the pH was adjusted to 5.0, 5.5, 6.0, or 6.5.

**Membrane Isolation and Western Blot Analysis.** Ten milliliters of midlog cells grown as they were for transport assays were harvested by centrifugation (5000g for 10 min). The pellet was resuspended in cell lysis buffer [50 mM TES (pH 8.0), 100 mM NaCl, 5 mM  $\beta$ -mercaptoethanol, 0.1 mg/mL TPCK, 0.7  $\mu\text{g/mL}$  pepstatin, and 25  $\mu\text{g/mL}$  PMSF] and quickly frozen in liquid nitrogen and thawed three times. The cell suspension was then sonicated three times for 20 s each. The membrane fraction was harvested by ultracentrifugation (45000 rpm for 45 min), and the pellet was resuspended in 200  $\mu\text{L}$  of extraction buffer

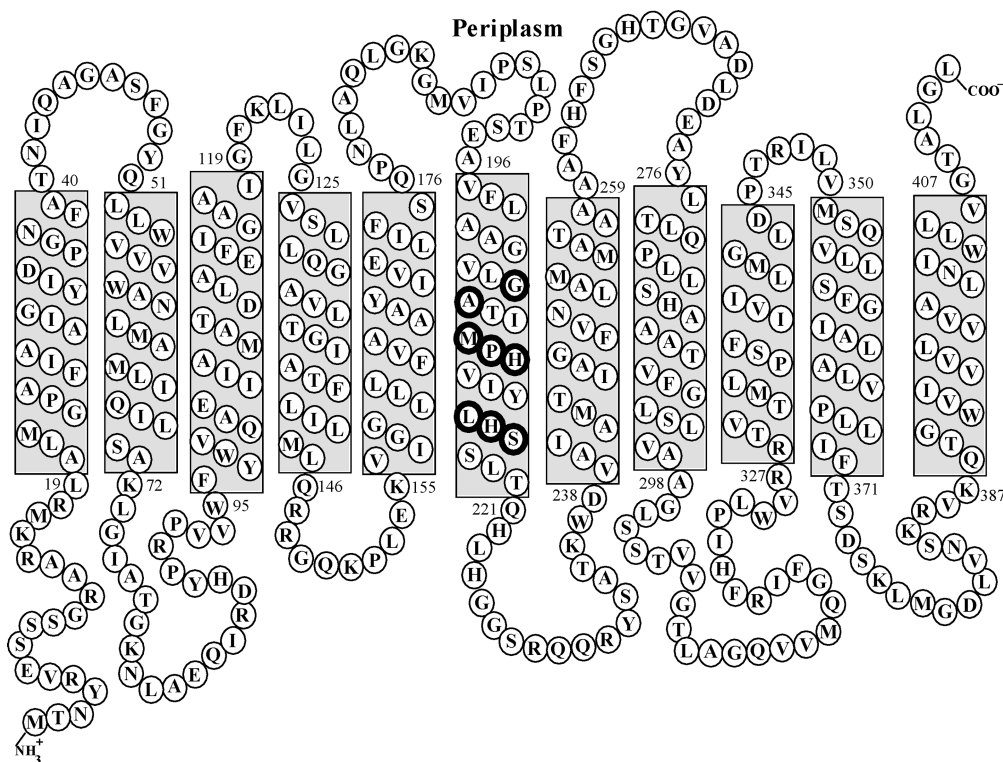


FIGURE 1: Secondary structure topology model of the *E. coli* Nramp homologue, MntH. Conserved residues mutated in this study are shown with darkened circles. This model was generated as previously described (1).

[50 mM TES (pH 8.0), 100 mM NaCl, 250 mM imidazole, 20% glycerol, 5 mM  $\beta$ -mercaptoethanol, and 0.05% lauryl maltoside]. Protein concentrations were determined using a modified Bradford assay (Bio-Rad). Samples of protein (50  $\mu$ g) were subjected to SDS-polyacrylamide gel electrophoresis, and Western blot analysis was performed using the method of Sambrook et al. (29). The primary polyclonal antibody recognizes the RGS-6H tag (Qiagen). The secondary antibody, goat anti-mouse conjugated to alkaline phosphatase, was purchased from Sigma. The Western blot was then scanned using a Molecular Dynamics laser densitometer and analyzed by comparison to wild-type values for the same preparation and Western blot. As shown in Table 1, the values for each mutant are reported as a percentage of wild-type 6HMntH averaged from three separate preparations.

**Kinetic Calculations.** For all mutant strains tested, apparent  $K_m$  and  $V_{max}$  values for  $^{54}\text{Mn}^{2+}$  transport were determined by observation of initial linear rates of transport at five external manganese concentrations (final  $\text{Mn}^{2+}$  concentrations of 0.1, 0.2, 0.3, 0.5, and 1.0  $\mu\text{M}$ ). A minimum of six transport measurements at each of the five concentrations were taken for all of the mutant strains. For the wild-type strains (pMntH and p6HMntH), the data were linear to 60 s. For wild-type and mutant strains with high activity, 30 and 60 s data points were taken in triplicate in three independent experiments. Thus, the data at each  $\text{Mn}^{2+}$  concentration were based on 18 data points. Certain mutants with lower levels of transport exhibited linear uptake for longer time periods, so kinetic measurements in these cases included data at 3 min in addition to the 30 and 60 s data points. Because the pH is constant, the transport velocity follows Michaelis-Menten kinetics with respect to  $^{54}\text{Mn}^{2+}$  concentration (30). Initial estimates of  $K_m$  were made using final  $\text{Mn}^{2+}$  concentrations of 0.2, 0.5, 1, 2.5, and 5.0  $\mu\text{M}$ , and the concentrations of  $\text{Mn}^{2+}$  used were readjusted to be 3-fold above and below the estimated  $K_m$  value. Results were calculated by an analysis of a

plot of  $v$  versus  $[S]$  using the graphic analysis program Excel (Microsoft). Data from three independent runs (each conducted in triplicate) were averaged to give a value for the apparent  $K_m$  and  $V_{max} \pm$  the standard error of the mean.

## RESULTS

**Identification of Conserved Residues in TMS-6.** Our proposed secondary structural model for *E. coli* MntH is shown in Figure 1 (1). This model agrees with the proposed topology from another study (11). Conserved residues of TMS-6 were determined as previously described for the conserved acidic residues of the Nramp family (1). The most highly conserved residues in TMS-6 were Gly-205, Ala-206, Met-209, Pro-210, His-211, Leu-215, His-216, and Ser-217. These residues are indicated by a darkened circle in Figure 1. On the basis of a BLAST search, all of these residues, except Leu-219, were 100% conserved among the top 100 homologues in the nonredundant database. (One homologue had Leu-219 changed to a methionine.) Such a high level of conservation is consistent with an important role of these residues with regard to structure and/or function.

**Mutagenesis of Conserved Histidine Residues.** Because MntH is an  $\text{H}^+/\text{Mn}^{2+}$  symporter, it is reasonable to postulate that the two highly conserved histidine residues might play a role in the binding of  $\text{Mn}^{2+}$  and/or  $\text{H}^+$ . To investigate this possibility, the conserved histidine residues (His-211 and His-216) were first changed to nonionizable residues of a similar size (i.e., histidine to glutamine). The histidines were also changed to a residue with a smaller side chain (alanine) and a larger ionizable residue (arginine). In some metal binding proteins, cysteine residues have been shown to substitute in metal binding for histidines (31–34), so the histidine residues were also changed to cysteine. The codon changes are described in Table 1. As seen in this table, the



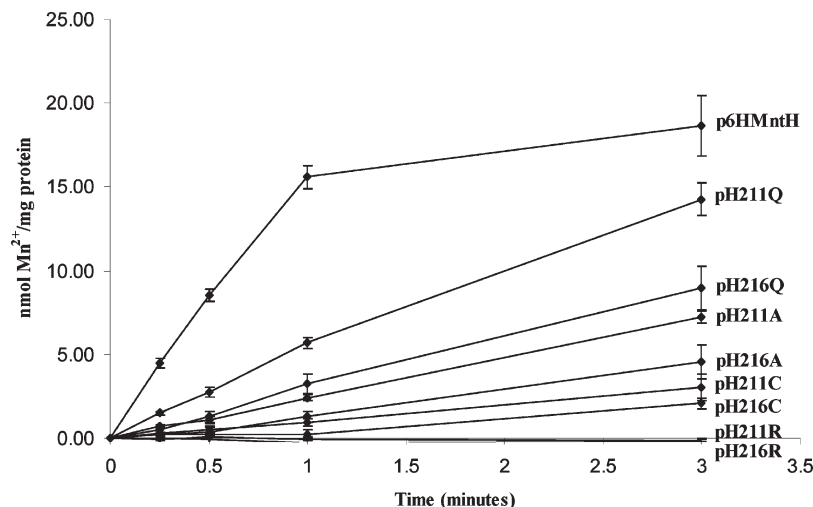


FIGURE 2: Transport characterization of wild-type and histidine mutants. The transport of  $^{54}\text{Mn}^{2+}$  was assessed at an external concentration of  $0.3\ \mu\text{M}$  at  $37\ ^\circ\text{C}$  as described in Materials and Methods.

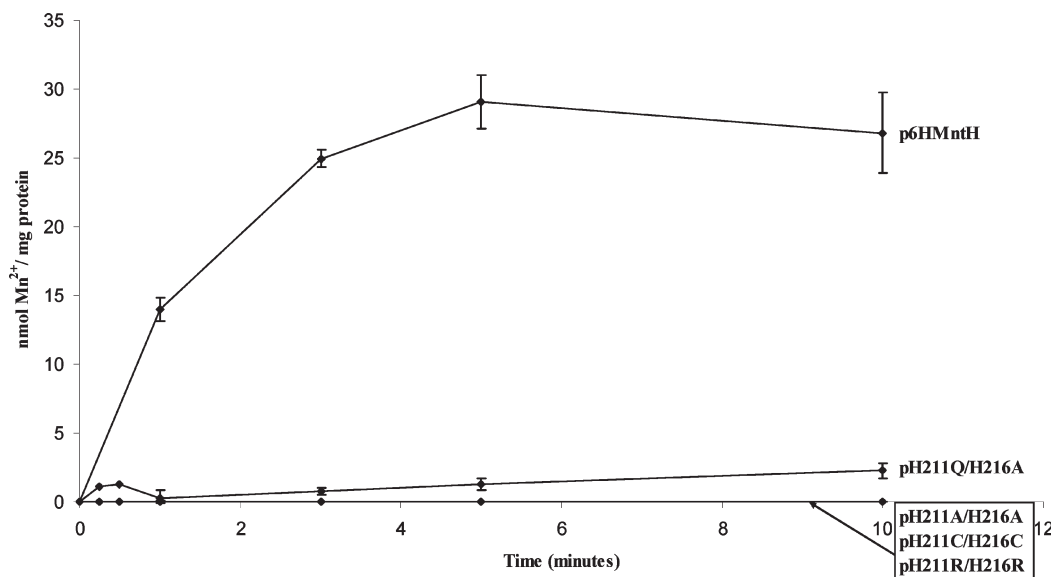


FIGURE 3: Transport characterization of wild-type MntH and double histidine MntH mutants. The transport of  $^{54}\text{Mn}^{2+}$  was assessed at an external concentration of  $0.3\ \mu\text{M}$  at  $37\ ^\circ\text{C}$  as described in Materials and Methods.

mutants were expressed at moderate to normal levels relative to the wild-type level.

Paired histidine residues have been reported to coordinate metals (24–26). To determine if metal transport could occur in the absence of these two highly conserved histidine residues, double mutations were also created. Each histidine was mutated to the same residue (e.g., H211Q/H216Q) via a second round of mutagenesis using a His-211 mutant as the template (see Table 1). Each double mutant was expressed at moderate to normal levels.

**Transport Characterization of Wild-Type, His-211 Mutant, and His-216 Mutant Strains.** The mutant strains were initially tested for  $^{54}\text{Mn}^{2+}$  uptake at  $0.3\ \mu\text{M}$ , which is the  $K_m$  value for the wild-type strain (1). Figure 2 shows the transport levels of the mutants involving the conserved histidine residues (positions 211 and 216). The H211Q strain transported  $\text{Mn}^{2+}$  to levels near 90% of that of the wild-type strain, whereas the H216Q strain transported it to levels roughly two-thirds of that of the wild-type strain. In addition, a few other mutants transported  $\text{Mn}^{2+}$  at detectable rates, but at a rate less than 25% of the wild-type rate. These included H211A, H216A, H211C, and H216C.

The remaining mutants (H211R and H216R) exhibited transport rates that were indistinguishable from the background levels of transport seen in the knockout strain.

Because alteration of just one of the two histidine residues still showed significant  $\text{Mn}^{2+}$  transport, it was of interest to assess the effect of a double histidine mutation in TMS-6. Therefore, both His-211 and His-216 were mutated to the same residue (e.g., H211Q/H216Q), and each of the four double mutants was tested for  $\text{Mn}^{2+}$  uptake. Three of the double mutants exhibited transport of  $\text{Mn}^{2+}$  indistinguishable from the background, but the H211Q/H216Q double mutant still transported  $\text{Mn}^{2+}$  at very low levels but reliably above the background (Figure 3).

To further investigate the importance of the histidine residues in TMS-6, the mutants with measurable levels of transport were examined with regard to the kinetics of  $^{54}\text{Mn}^{2+}$  uptake. These results are presented in Table 2. The H211Q strain had a moderately high  $V_{\max}$  value and a  $K_m$  value that was not significantly different from that of the wild-type strain. Thus, it appears that His-211 is not critical for cation binding or transport. By comparison, the other mutants tested showed  $V_{\max}$

Table 2: Kinetic Characterization of the Wild Type and Substitutions of the Conserved Histidine Residues

strain	apparent $K_m^a \pm \text{SEM}$ ( $\mu\text{M}$ )	apparent $V_{\text{max}}^a \pm \text{SEM}$ ( $\text{nmol mg}^{-1} \text{min}^{-1}$ )
6HMnH (wild type)	$0.3 \pm 0.1$	$19.2 \pm 7.2$
H211A	$0.3 \pm 0.1$	$4.1 \pm 0.1$
H211C	$0.3 \pm 0.1$	$2.6 \pm 0.7$
H211Q	$0.2 \pm 0.1$	$8.1 \pm 0.8$
H216A	$0.2 \pm 0.0$	$1.7 \pm 0.2$
H216C	$0.7 \pm 0.1$	$3.4 \pm 0.0$

<sup>a</sup>Kinetics measurements were taken as described in Materials and Methods.

values that were less than 25% of that of the wild-type strain. All mutant strains tested (H211A, H211C, and H216A), except H216C, had  $K_m$  values similar to that of the wild type. The H216C strain had a slightly elevated  $K_m$  of  $0.7 \mu\text{M}$ . It is possible that having a cysteine side chain in this position affected the overall tertiary structure of MntH, lowering the affinity for  $\text{Mn}^{2+}$  in the metal binding site. Additional supporting evidence for a disruption in overall structure by the cysteine substitution rather than direct interference with the metal binding site is shown by H216A having a  $K_m$  similar to that of the wild type.

A study from the Gros laboratory indicated that the two conserved histidines (His-267 and His-272) in mammalian Nramp2 play a role in the pH regulation of metal transport function. It was found that alanine and cysteine substitutions, which had low activity at pH 6.0, were substantially rescued by lowering the pH (20). To determine if the homologous conserved histidine residues in the MntH protein from *E. coli* also played such a role, we examined the transport of two single mutants, H211Q and H216Q, and the corresponding double mutant at pH 5.0, 5.5, 6.0, and 6.5 (Figures 4 and 5). With regard to position 211, there was an increase in transport function from pH 6.5 to 5.0. However, the degree of change was not as dramatic as that seen in the mammalian protein in which transport function was very low at pH 6.0 and 6.5 (see ref 20). For position 216, transport function changed in the opposite direction with the highest activity, relative to the wild-type strain, observed at pH 6.5.

**Mutagenesis of Other Conserved Residues along TMS-6.** Certain residues surrounding the histidine pair (Gly-205, Ala-206, Met-209, Pro-210, Leu-215, and Ser-217) are also highly conserved throughout the Nramp family. To investigate their role in structure and function, each was changed to a variety of other residues, some substitutions preserving size of the side chain (i.e., Leu to Ile) and other substitutions changing the side chain size or chemistry (i.e., Met to Lys or Ser to Tyr). All mutations made to these sites are listed in Table 1. All mutations were expressed at moderate to normal levels compared to the level of wild-type expression.

**Transport Characterization of Mutants Surrounding the Histidine Pair.** The mutants at positions 205, 206, 209, 210, 215, and 217 were tested for  $\text{Mn}^{2+}$  transport at  $0.3 \mu\text{M}$   $\text{Mn}^{2+}$  (see Figures 6 and 7). Mutation of Gly-205 to Ala showed low levels of transport, whereas a mutation to Pro was completely defective. It should be noted that for all mutants not showing transport activity during the initial testing, further transport experiments were extended to 10 min to confirm the lack of  $\text{Mn}^{2+}$  transport activity. Preserving a smaller side chain volume as in the case of the A206G mutation caused a 50% decrease in transport activity, while substitution of a larger residue, leucine, abolished transport

activity. Substitution of neither Ile nor Lys for Met-209 showed transport activity, despite the similar side chain volumes of Met and Ile. Interestingly, mutation of Pro-210 to Gln or Ala decreased transport activity to 25% of wild-type activity, but mutation to a Gly abolished transport. Glycine has a smaller side chain volume than proline, but in our previous mutagenesis of Pro-37, substitution of a glycine was the only mutation in which transport activity was still observed (1).

Histidine 216 is flanked by two highly conserved residues, Leu-215 and Ser-217. A number of mutations were made to each of these residues, and the results are shown in Figure 7. Only the substitution of Ile to Leu still showed transport, albeit at low levels at 10 min, whereas changing the Leu to Ala or Val abolished transport. Of the four substitutions made to Ser-217, only S217T and S217A mutations had measurable levels of transport. Transport was abolished in the S217Q and S217Y mutants. Serine, threonine, and tyrosine all have similar side chain chemistry with a hydroxyl group, but serine and threonine are more similar in side chain volume, suggesting that preserving side chain volume is important to function at this position. Alanine is also fairly similar in side chain volume to serine, whereas glutamine is much larger.

Kinetic analyses were performed on selected mutants (Table 3). G205A had a much lower  $V_{\text{max}}$  than wild-type MntH and a slightly elevated  $K_m$  of  $0.7 \mu\text{M}$ . An indirect effect on metal binding is a probable cause of the elevated  $K_m$  considering the periplasmic end of TMS-6 may be positioned relatively close to the proposed binding site in the periplasmic ends of TMS-1–3. Mutation of glycine, a fairly small residue, to a slightly larger alanine may perturb the tertiary structure required for metal ion binding. Mutation of Gly-205 to an even larger residue, Pro, completely abolished transport. Kinetic measurements of P210A and P210Q were almost identical to each other, having a  $K_m$  similar to the wild-type value and a  $V_{\text{max}}$  that was approximately 20% of the wild-type MntH value. L215I, S217A, and S217T strains also all had  $K_m$  values similar to that of the wild type and  $V_{\text{max}}$  values much lower than that of the wild type: 1.3, 4.3, and  $4.3 \text{ nmol mg}^{-1} \text{min}^{-1}$ , respectively.

## DISCUSSION

In this study, we investigated the role of two conserved histidine residues, His-211 and His-216, in *E. coli* MntH. In other proteins, histidine residues have been shown to play critical roles in transporter function. In transport proteins that transport or sense hydrogen ions, histidines may be directly involved in  $\text{H}^+$  recognition (35, 36). Histidine residues have also been implicated in pH-dependent regulation or modulation of a number of transport and channel proteins. For example, a single histidine residue determines the pH sensitivity of the cardiac and neuronal channel, HCN2 (37). Also, a single histidine is important for the pH regulation of the cardiac gap-junction protein connexin (38). In addition, histidines within proteins are capable of forming intra- and intermolecular hydrogen bonds.

Other roles for histidine residues include substrate recognition and the interaction of helices during conformational changes. In the EAAC1 transporter (a glutamate/ $\text{H}^+$  symporter), a single histidine residue (His-295) was hypothesized to be the proton acceptor because mutation of this residue to Arg, Thr, and Asn led to a nonfunctional protein (39). However, a more recent study examined the effects of additional substitutions of His-295 via changes of this residue to Cys and Gln and revisitation of the

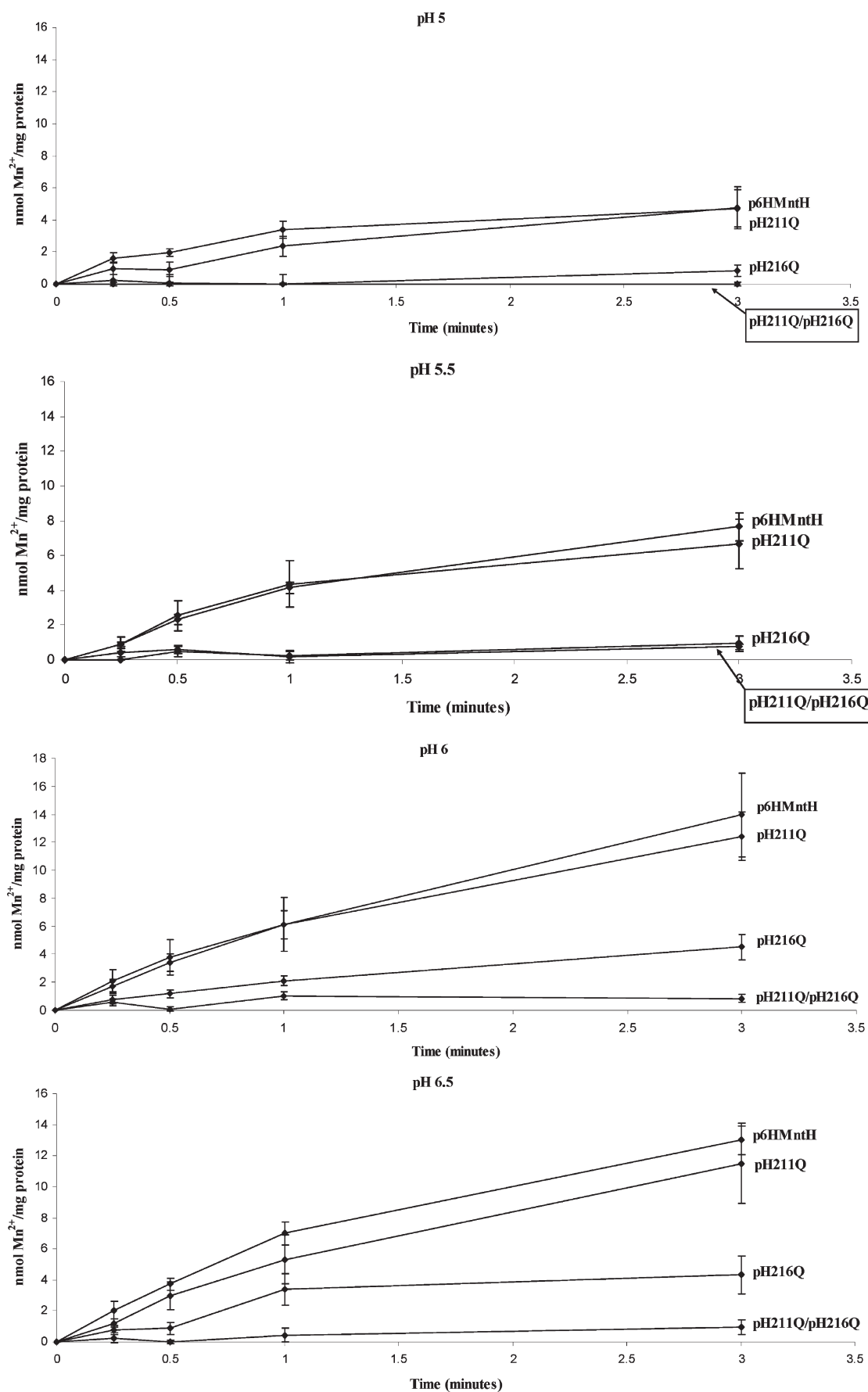


FIGURE 4: Transport characterization of the wild type and H211Q and H216Q mutants at pH 5.0–6.5. The transport of  $^{54}\text{Mn}^{2+}$  was assessed at an external concentration of  $0.3 \mu\text{M}$  at  $37^\circ\text{C}$  as described in Materials and Methods.

H295N mutation. H295N and H295C can still bind glutamate and  $\text{H}^+$  even though the protein has little to no transport

activity (40). Interestingly, substitution with glutamine maintained transport levels indistinguishable from the wild-type level.

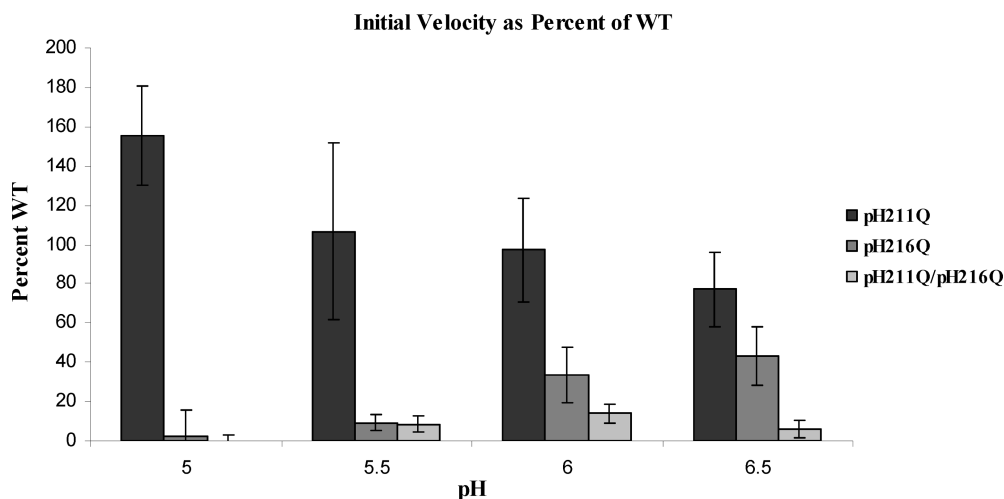


FIGURE 5: Relative transport rates of H211Q, H216Q, and H211Q/H216Q mutants at pH 5.0–6.5. The transport of  $^{54}\text{Mn}^{2+}$  was assessed at an external concentration of  $0.3\ \mu\text{M}$  at  $37^\circ\text{C}$  as described in Materials and Methods. Initial rates were determined and are expressed as a percentage of the wild-type rate at each pH.

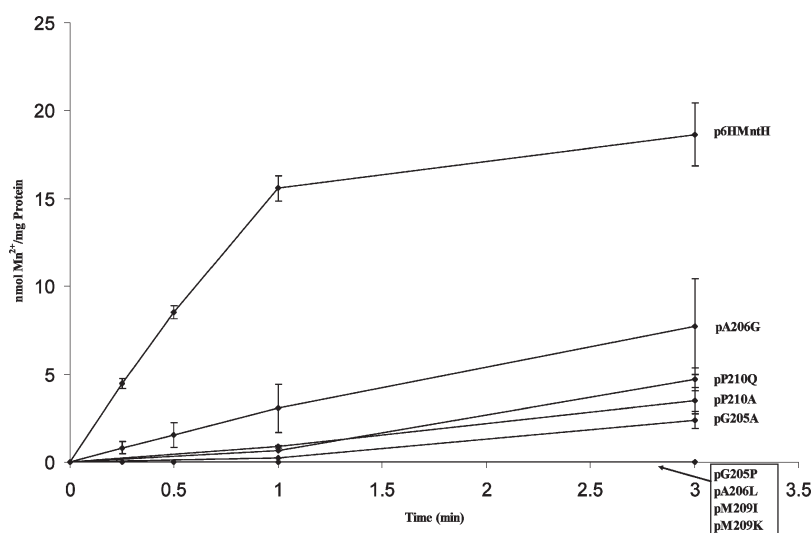


FIGURE 6:  $^{54}\text{Mn}^{2+}$  uptake in wild-type and mutant strains that have alterations to conserved residues: Gly-205, Ala-206, Met-209, and Pro-210. The transport of  $^{54}\text{Mn}^{2+}$  was assessed at an external concentration of  $0.3\ \mu\text{M}$  at  $37^\circ\text{C}$  as described in Materials and Methods.

This suggested that His-295 is not protonated at physiological pH and does not contribute to proton transport. It appears that the side chain volume and/or length of His-295 is important for preserving the overall protein structure or conformational changes that occur during transport. In addition, Gln can substitute for the NH ( $\epsilon$ ) group of the histidine ring, acting as a hydrogen bond donor (41). His-295 may act as a hydrogen donor to an unidentified acceptor, and this interaction may be critical for function. This would explain the ability of Gln to substitute for His without affecting protein function.

The conserved histidine residues mutated in our study have also been investigated in the mouse Nramp2 homologue. The Gros laboratory examined the effects of mutating the histidine pair in TMS-6 (20). His-267 (equivalent to *E. coli* His-211) and His-272 (*E. coli* His-216) were each changed to alanine, cysteine, and arginine, and double mutants were also created. They found all mutants except H267C/H272C to be stably expressed in the membrane when expressed in a yeast double mutant (*smf1/smf2*) strain and when transfected into CHO cells. Each mutation was tested for  $\text{Fe}^{2+}$  and  $\text{Co}^{2+}$  (pH 6.0) transport in CHO cells. H267A, H267R, H272R, H267A/H272A, and H267R/H272R

were all inactive for transport in both cases. Only H267A and H272C had significant transport activity compared to wild-type Nramp2. When the pH of the assay was lowered to 5.0, wild-type Nramp2 maintained the same level of transport activity for  $\text{Fe}^{2+}$  and  $\text{Co}^{2+}$  but H267A, H267C, and H272C exhibited increased transport activity at the lower pH, whereas H272A and H267A/H272A, which had been inactive at pH 6.0, were rescued at lower pH levels. They also made the observation that His-267 was more sensitive to mutation than His-272. The authors suggested that the histidine pair may be involved in the pH regulation of transport. In another study, Mackenzie et al. monitored metal ion uptake, currents, and intracellular pH in the wild type and histidine mutants of rat Nramp2 expressed in *Xenopus* oocytes (42). They concluded that His-272 (equivalent to His-216 in *E. coli* MntH) is critical for coupling of metal ion transport to  $\text{H}^+$  transport. Mutation of His-272 to alanine or arginine disrupted the coupling observed in wild-type Nramp2.

With regard to MntH in *E. coli*, Chaloupka et al. mutated both of the histidine residues (His-211 and His-216) in *E. coli* MntH (21). Several different single mutations were introduced (H211Y, H211A, H216A, and H216R), but no double mutants

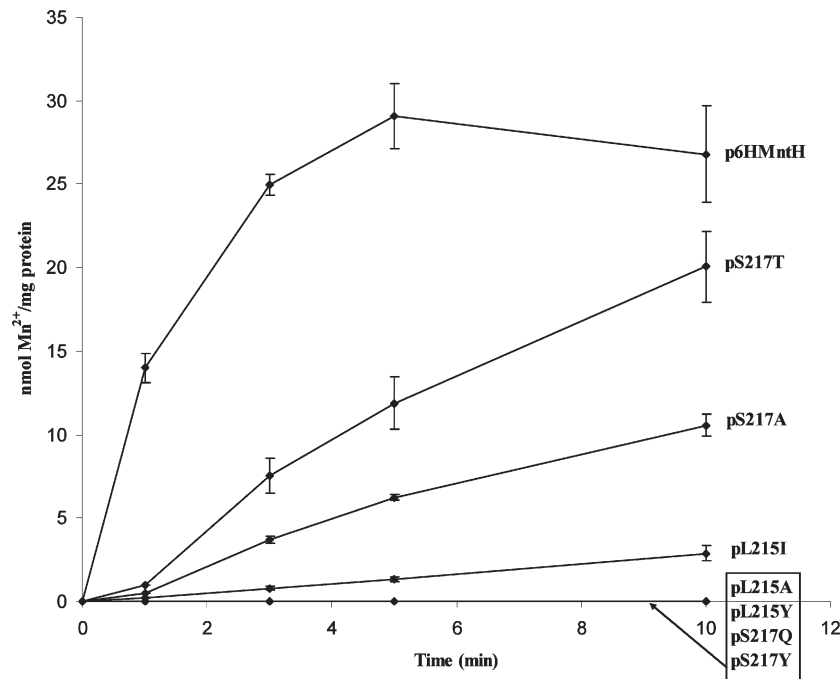


FIGURE 7:  $^{54}\text{Mn}^{2+}$  uptake in 6-His wild-type and mutant strains that have alterations to conserved residues: Leu-215 and Ser-217. The transport of  $^{54}\text{Mn}^{2+}$  was assessed at an external concentration of  $0.3\ \mu\text{M}$  at  $37\ ^\circ\text{C}$  as described in Materials and Methods.

were introduced. The tyrosine mutation was chosen on the basis of the results of their evolutionary analysis of the Nramp family. Tyrosine is the most prevalent substitution for His-211 in the phylogenetic outgroup. In terms of size and hydrophobicity, it is a conservative substitution, but tyrosine exposes an acidic proton instead of the basic imidazole group of histidine. Sensitivity to metals was reduced in H211Y, and no transport was detected with  $\text{Mn}^{2+}$ , although cotransport of  $\text{Cd}^{2+}$  and  $\text{H}^+$  was detected at low levels. H211A preserved metal sensitivity (but was not as sensitive as the wild type) and demonstrated transport of  $\text{H}^+$  and  $\text{Cd}^{2+}$ ,  $\text{Fe}^{2+}$ , and  $\text{Mn}^{2+}$  at pH 4.7. The authors concluded that His-211 is structurally and functionally important. However, it was not found to be essential because some activity was maintained with both mutations to His-211. Mutation of His-216 to Ala preserved the transport activity of metal ions and  $\text{H}^+$ , but changing this residue to Arg abolished transport activity. H211A was observed to be less sensitive to mutation than H216A, which is the opposite of what was observed with mouse Nramp2 (20). In a more recent study, a H211Y mutant in MntH was shown to have an elevated  $K_m$  value and negligible transport at pH 7.5, indicating that position 211 may be important for both metal binding and pH dependence (23).

However, our results indicate that His-211 and His-216 do not play a critical role in metal binding. Substitutions at these sites had  $K_m$  values that were similar to that of the wild-type strain (see Table 3). Also, our results do not suggest a major role of His-211 or His-216 with regard to pH regulation of metal transport. At position 211, the H211Q mutant exhibited a modest increase in transport function from pH 6.5 to 5.0. However, the degree of change was not as dramatic as that seen in the mammalian protein in which the transport function activity of certain mutants was very low at pH 6.0 and 6.5 (see ref 20). For the H216Q mutant, transport function changed in the opposite direction with the highest activity, relative to the wild-type strain, observed at pH 6.5. Taken together, our results do not strongly support a role of the conserved histidine residues with regard to

Table 3: Kinetic Characterization of the Wild Type and Substitutions of the Other Conserved Residues

strain	apparent $K_m \pm \text{SEM}$ ( $\mu\text{M}$ )	apparent $V_{\text{max}}^a \pm \text{SEM}$ ( $\text{nmol mg}^{-1} \text{min}^{-1}$ )
6HMntH (wild type)	$0.3 \pm 0.1$	$19.2 \pm 7.2$
G205A	$0.7 \pm 0.2$	$3.6 \pm 0.3$
P210A	$0.3 \pm 0.1$	$2.6 \pm 0.3$
P210Q	$0.3 \pm 0.1$	$3.9 \pm 0.9$
L215I	$0.2 \pm 0.0$	$1.3 \pm 0.3$
S217A	$0.3 \pm 0.1$	$4.3 \pm 1.4$
S217T	$0.1 \pm 0.0$	$4.3 \pm 0.1$

<sup>a</sup>Kinetics measurements were taken as described in Materials and Methods.

pH regulation of the transporter. Instead, the effects of side chain volume changes are consistent with a role in conformational changes associated with transport. The glutamine substitutions had the highest levels of transport, and this residue is the closest in side chain volume to histidine. Arginine is a larger side chain than histidine, and the increase in size in these positions (211 and 216) abolished  $\text{Mn}^{2+}$  transport. Likewise, cysteine and alanine are smaller, and replacing His-211 or His-216 with this residue decreased transport activity.

Similarly, the other conserved residues (G205, A206, M209, P210, L215, and S217) seem to be important for transport function but do not seem to be directly involved in metal binding. In all cases, mutations at these sites had apparent  $K_m$  values that were similar to that of the wild-type strain but  $V_{\text{max}}$  values that were substantially reduced. Those substitutions with side chain volumes most similar to that of the wild-type residue tended to have the highest activities.

Translocation of substrates by secondary active transporters requires conformational changes that promote conversion between an outwardly accessible and an inwardly accessible substrate binding site (43, 44). Crystal structures of other secondary active transporters show that the helices surround a central cavity



perpendicular to the plane of the membrane and a pseudo-2-fold symmetry is observed in the folding of the helices into their tertiary structure (45–48). In the case of the glycerol 3-phosphate transporter from *E. coli*, each half of the protein forms two 3-helix bundles (46). This arrangement has been observed with other membrane transport proteins. A “rocker-switch” type of motion of transmembrane helices during substrate transport has been proposed on the basis of modeling with the crystal structure for the glycerol 3-phosphate transporter and other transporters with determined crystal structures (46–48). At the interface between the two “halves” of the protein, the periplasmic ends of the helices would separate as their cytoplasmic ends come together. Movements of the helices and their side chains are necessary for this rocker-switch motion to occur.

The conserved residues identified in this study could potentially lie on a face or faces of TMS-6 in MntH and be indispensable for function without playing a specific role in  $Mn^{2+}$  or  $H^{+}$  binding. This idea could be further tested by directly measuring the binding of  $Mn^{2+}$  to the wild-type or mutant proteins. If mutations in TMS-6 that inhibit transport do not have a direct effect on metal binding, such an observation would be consistent with their role in conformational changes.

Critically important faces of transmembrane helices have been identified in the lactose permease prior to the availability of a crystal structure. Site-directed mutagenesis studies of loop 2/3 and TMS-2 of lactose permease suggested that the topology of TMS-2 is important for the function and stability of the lactose permease (49–52). A similar observation was made with regard to loop 8/9 and TMS-8 of the lactose permease, suggesting structural symmetry between the two halves of the protein before the symmetry was confirmed by crystallography studies (53–57). In TMS-8 of lactose permease, mutations along one face have detrimental effects on the initial rate of lactose transport and the maximal velocity of transport without significantly affecting the apparent  $K_m$  values for lactose binding when the mutation alters the side chain volume of the residues (53). Likewise, in our study, the effects of mutating conserved residues along TMS-6 could be interpreted as having a negative impact on a conformationally sensitive interface in MntH.

## REFERENCES

- Haemig, H. A., and Brooker, R. J. (2004) Importance of conserved acidic residues in MntH, the Nramp homolog of *Escherichia coli*. *J. Membr. Biol.* 201 (2), 97–107.
- Vidal, S. M., Malo, D., Vogan, K., Skamene, E., and Gros, P. (1993) Natural resistance to infection with intracellular parasites: Isolation of a candidate for Bcg. *Cell* 73 (3), 469–485.
- Gunshin, H., Mackenzie, B., Berger, U. V., Gunshin, Y., Romero, M. F., Boron, W. F., Nussberger, S., Gollan, J. L., and Hediger, M. A. (1997) Cloning and characterization of a mammalian proton-coupled metal-ion transporter. *Nature* 388 (6641), 482–488.
- Mulero, V., Searle, S., Blackwell, J. M., and Brock, J. H. (2002) Solute carrier 11a1 (Slc11a1; formerly Nramp1) regulates metabolism and release of iron acquired by phagocytic, but not transferrin-receptor-mediated, iron uptake. *Biochem. J.* 363 (Part 1), 89–94.
- Forbes, J. R., and Gros, P. (2001) Divalent-metal transport by NRAMP proteins at the interface of host-pathogen interactions. *Trends Microbiol.* 9 (8), 397–403.
- Papp-Wallace, K. M., and Maguire, M. E. (2006) Manganese transport and the role of manganese in virulence. *Annu. Rev. Microbiol.* 60, 187–209.
- Anderson, E. S.; et al. (2009) The Manganese Transporter MntH Is a Critical Virulence Determinant for *Brucella abortus* 2308 in Experimentally Infected Mice. *Infect. Immun.* 77, 3466–3474.
- Cellier, M., Prive, G., Belouchi, A., Kwan, T., Rodrigues, V., Chia, W., and Gros, P. (1995) Nramp defines a family of membrane proteins. *Proc. Natl. Acad. Sci. U.S.A.* 92 (22), 10089–10093.
- Makui, H., Roig, E., Cole, S. T., Helmann, J. D., Gros, P., and Cellier, M. F. (2000) Identification of the *Escherichia coli* K-12 Nramp orthologue (MntH) as a selective divalent metal ion transporter. *Mol. Microbiol.* 35 (5), 1065–1078.
- Kehres, D. G., Zaharik, M. L., Finlay, B. B., and Maguire, M. E. (2000) The NRAMP proteins of *Salmonella typhimurium* and *Escherichia coli* are selective manganese transporters involved in the response to reactive oxygen. *Mol. Microbiol.* 36 (5), 1085–1100.
- Courville, P., Chaloupka, R., and Cellier, M. F. (2006) Recent progress in structure-function analyses of Nramp proton-dependent metal-ion transporters. *Biochem. Cell Biol.* 84 (6), 960–978.
- Silver, S., Johnseine, P., and King, K. (1970) Manganese active transport in *Escherichia coli*. *J. Bacteriol.* 104 (3), 1299–1306.
- Courville, P., Chaloupka, R., Veyrier, F., and Cellier, M. F. (2004) Determination of transmembrane topology of the *Escherichia coli* natural resistance-associated macrophage protein (Nramp) ortholog. *J. Biol. Chem.* 279 (5), 3318–3326.
- Fleming, M. D., Trenor, C. C., III, Su, M. A., Foerzler, D., Beier, D. R., Dietrich, W. F., and Andrews, N. C. (1997) Microcytic anaemia mice have a mutation in Nramp2, a candidate iron transporter gene. *Nat. Genet.* 16 (4), 383–386.
- Fleming, M. D., Romano, M. A., Su, M. A., Garrick, L. M., Garrick, M. D., and Andrews, N. C. (1998) Nramp2 is mutated in the anemic Belgrade (b) rat: Evidence of a role for Nramp2 in endosomal iron transport. *Proc. Natl. Acad. Sci. U.S.A.* 95 (3), 1148–1153.
- Su, M. A., Trenor, C. C., Fleming, J. C., Fleming, M. D., and Andrews, N. C. (1998) The G185R mutation disrupts function of the iron transporter Nramp2. *Blood* 92 (6), 2157–2163.
- Blackwell, J. M., Searle, S., Mohamed, H., and White, J. K. (2003) Divalent cation transport and susceptibility to infectious and autoimmune disease: Continuation of the Ity/Lsh/Bcg/Nramp1/Slc11a1 gene story. *Immunol. Lett.* 85 (2), 197–203.
- Patruta, S. I., and Horl, W. H. (1999) Iron and infection. *Kidney Int. Suppl.* 69, S125–S130.
- Ratledge, C., and Dover, L. G. (2000) Iron metabolism in pathogenic bacteria. *Annu. Rev. Microbiol.* 54, 881–941.
- Lam-Yuk-Tseung, S., Govoni, G., Forbes, J., and Gros, P. (2003) Iron transport by Nramp2/DMT1: pH regulation of transport by 2 histidines in transmembrane domain 6. *Blood* 101 (9), 3699–3707.
- Chaloupka, R., Courville, P., Veyrier, F., Knudsen, B., Tompkins, T. A., and Cellier, M. F. (2005) Identification of functional amino acids in the Nramp family by a combination of evolutionary analysis and biophysical studies of metal and proton cotransport in vivo. *Biochemistry* 44 (2), 726–733.
- Cohen, A., Nevo, Y., and Nelson, N. (2003) The first external loop of the metal ion transporter DCT1 is involved in metal ion binding and specificity. *Proc. Natl. Acad. Sci. U.S.A.* 100 (19), 10694–10699.
- Courville, P., Urbankova, E., Rensing, C., Chaloupka, R., Quick, M., and Cellier, M. F. (2008) Solute carrier 11 cation symport requires distinct residues in transmembrane helices 1 and 6. *J. Biol. Chem.* 283 (15), 9651–9658.
- Eicken, C., Pennella, M. A., Chen, X., Koshlap, K. M., VanZile, M. L., Sacchettini, J. C., and Giedroc, D. P. (2003) A metal-ligand-mediated intersubunit allosteric switch in related SmtB/ArzR zinc sensor proteins. *J. Mol. Biol.* 333 (4), 683–695.
- Voss, J., Hubbell, W. L., and Kaback, H. R. (1995) Distance determination in proteins using designed metal ion binding sites and site-directed spin labeling: Application to the lactose permease of *Escherichia coli*. *Proc. Natl. Acad. Sci. U.S.A.* 92 (26), 12300–12303.
- Eng, B. H., Guerinot, M. L., Eide, D., and Saier, M. H., Jr. (1998) Sequence analyses and phylogenetic characterization of the ZIP family of metal ion transport proteins. *J. Membr. Biol.* 166 (1), 1–7.
- Kraft, R., Tardiff, J., Krauter, K. S., and Leinwand, L. A. (1998) Using mini-prep plasmid DNA for sequencing double stranded templates with Sequenase. *BioTechniques* 6 (6), 544–547.
- Martinez, E., Bartolome, B., and de la Cruz, F. (1988) pACYC184-derived cloning vectors containing the multiple cloning site and lacZ  $\alpha$  reporter gene of pUC8/9 and pUC18/19 plasmids. *Gene* 68 (1), 159–162.
- Sambrook, J., Fritsch, E. F., and Maniatis, T. (1989) Molecular Cloning: A Laboratory Manual, Cold Spring Harbor Laboratory Press, Plainview, NY.
- Segel, I. (1975) Enzyme Kinetics, Wiley-Interscience, New York.
- Nakagama, H., Heinrich, G., Pelletier, J., and Housman, D. E. (1995) Sequence and structural requirements for high-affinity DNA binding by the WT1 gene product. *Mol. Cell. Biol.* 15 (3), 1489–1498.
- Omichinski, J. G., Trainor, C., Evans, T., Gronenborn, A. M., Clore, G. M., and Felsenfeld, G. (1993) A small single-“finger” peptide from the erythroid transcription factor GATA-1 binds specifically to DNA

- as a zinc or iron complex. *Proc. Natl. Acad. Sci. U.S.A.* 90 (5), 1676–1680.
33. Ghazaleh, F. A., Omburo, G. A., and Colman, R. W. (1996) Evidence for the presence of essential histidine and cysteine residues in platelet cGMP-inhibited phosphodiesterase. *Biochem. J.* 317 (Part 2), 495–501.
34. Worthington, M. T., Amann, B. T., Nathans, D., and Berg, J. M. (1996) Metal binding properties and secondary structure of the zinc-binding domain of Nup475. *Proc. Natl. Acad. Sci. U.S.A.* 93 (24), 13754–13759.
35. Chen, X. Z., Steel, A., and Hediger, M. A. (2000) Functional roles of histidine and tyrosine residues in the  $H^+$ -peptide transporter PepT1. *Biochem. Biophys. Res. Commun.* 272 (3), 726–730.
36. Wiebe, C. A., Dibattista, E. R., and Fliegel, L. (2001) Functional role of polar amino acid residues in  $Na^+/H^+$  exchangers. *Biochem. J.* 357 (Part 1), 1–10.
37. Zong, X., Stieber, J., Ludwig, A., Hofmann, F., and Biel, M. (2001) A single histidine residue determines the pH sensitivity of the pacemaker channel HCN2. *J. Biol. Chem.* 276 (9), 6313–6319.
38. Ek, J. F., Delmar, M., Perzova, R., and Taffet, S. M. (1994) Role of histidine 95 on pH gating of the cardiac gap junction protein connexin43. *Circ. Res.* 74 (6), 1058–1064.
39. Zhang, Y., Pines, G., and Kanner, B. I. (1994) Histidine 326 is critical for the function of GLT-1, a ( $Na^+ + K^+$ )-coupled glutamate transporter from rat brain. *J. Biol. Chem.* 269 (30), 19573–19577.
40. Tao, Z., and Grewer, C. (2005) The conserved histidine 295 does not contribute to proton cotransport by the glutamate transporter EAAC1. *Biochemistry* 44 (9), 3466–3476.
41. Fersht, A. (1999) Structure and mechanism in protein science: A guide to enzyme catalysis and protein folding, Vol. xxi, p 631, W. H. Freeman, New York.
42. Mackenzie, B., Ujwal, M. L., Chang, M. H., Romero, M. F., and Hediger, M. A. (2006) Divalent metal-ion transporter DMT1 mediates both  $H^+$ -coupled  $Fe^{2+}$  transport and uncoupled fluxes. *Pfluegers Arch.* 451 (4), 544–558.
43. West, I. C. (1997) Ligand conduction and the gated-pore mechanism of transmembrane transport. *Biochim. Biophys. Acta* 1331 (3), 213–234.
44. Tanford, C. (1983) Translocation pathway in the catalysis of active transport. *Proc. Natl. Acad. Sci. U.S.A.* 80 (12), 3701–3705.
45. Hunte, C., Screpanti, E., Venturi, M., Rimón, A., Padan, E., and Michel, H. (2005) Structure of a  $Na^+/H^+$  antiporter and insights into mechanism of action and regulation by pH. *Nature* 435 (7046), 1197–1202.
46. Huang, Y., Lemieux, M. J., Song, J., Auer, M., and Wang, D. N. (2003) Structure and mechanism of the glycerol-3-phosphate transporter from *Escherichia coli*. *Science* 301 (5633), 616–620.
47. Faham, S., Watanabe, A., Besserer, G. M., Cascio, D., Specht, A., Hirayama, B. A., Wright, E., and Abramson, J. (2008) The Crystal Structure of a Sodium Galactose Transporter Reveals Mechanistic Insights into  $Na^+$ /Sugar Symport. *Science* 321, 810–813.
48. Abramson, J., Smirnova, I., Kasho, V., Verner, G., Kaback, H. R., and Iwata, S. (2003) Structure and mechanism of the lactose permease of *Escherichia coli*. *Science* 301 (5633), 610–615.
49. Jessen-Marshall, A. E., Paul, N. J., and Brooker, R. J. (1995) The conserved motif, GXXX(D/E)(R/K)XG[X](R/K)(R/K), in hydrophilic loop 2/3 of the lactose permease. *J. Biol. Chem.* 270 (27), 16251–16257.
50. Jessen-Marshall, A. E., and Brooker, R. J. (1996) Evidence that transmembrane segment 2 of the lactose permease is part of a conformationally sensitive interface between the two halves of the protein. *J. Biol. Chem.* 271 (3), 1400–1404.
51. Jessen-Marshall, A. E., Parker, N. J., and Brooker, R. J. (1997) Suppressor analysis of mutations in the loop 2–3 motif of lactose permease: Evidence that glycine-64 is an important residue for conformational changes. *J. Bacteriol.* 179 (8), 2616–2622.
52. Green, A. L., Anderson, E. J., and Brooker, R. J. (2000) A revised model for the structure and function of the lactose permease. Evidence that a face on transmembrane segment 2 is important for conformational changes. *J. Biol. Chem.* 275 (30), 23240–23246.
53. Green, A. L., and Brooker, R. J. (2001) A face on transmembrane segment 8 of the lactose permease is important for transport activity. *Biochemistry* 40 (40), 12220–12229.
54. Green, A. L., Hrodey, H. A., and Brooker, R. J. (2003) Evidence for structural symmetry and functional asymmetry in the lactose permease of *Escherichia coli*. *Biochemistry* 42 (38), 11226–11233.
55. Pazdernik, N. J., Jessen-Marshall, A. E., and Brooker, R. J. (1997) Role of conserved residues in hydrophilic loop 8–9 of the lactose permease. *J. Bacteriol.* 179 (3), 735–741.
56. Pazdernik, N. J., Cain, S. M., and Brooker, R. J. (1997) An analysis of suppressor mutations suggests that the two halves of the lactose permease function in a symmetrical manner. *J. Biol. Chem.* 272 (42), 26110–26116.
57. Pazdernik, N. J., Matzke, E. A., Jessen-Marshall, A. E., and Brooker, R. J. (2000) Roles of charged residues in the conserved motif, G-X-X-X-D/E-R/K-X-G-[X]-R/K-R/K, of the lactose permease of *Escherichia coli*. *J. Membr. Biol.* 174 (1), 31–40.